ResearchGate

See discussions, stats, and author profiles for this publication at: https://www.researchgate.net/publication/233932215

Computational Study on the Characteristics of the Interaction in Linear Urea Clusters

ARTICLE *in* INTERNATIONAL JOURNAL OF QUANTUM CHEMISTRY · OCTOBER 2011

Impact Factor: 1.43 · DOI: 10.1002/qua.22628

CITATIONS
23

READS
40

3 AUTHORS, INCLUDING:

Mehdi D Esrafili
University of Maragheh
179 PUBLICATIONS **899** CITATIONS
SEE PROFILE

Javad Beheshtian
Shahid Rajaee University
80 PUBLICATIONS **1,097** CITATIONS
SEE PROFILE

Available from: Mehdi D Esrafili
Retrieved on: 25 January 2016

Computational Study on the Characteristics of the Interaction in Linear Urea Clusters

MEHDI D. ESRAFILI,[1,2] JAVAD BEHESHTIAN,[2] NASSER L. HADIPOUR[2]

[1]*Fukui Institute for Fundamental Chemistry, Kyoto University, Kyoto, Japan*
[2]*Department of Chemistry, Tarbiat Modares University, Tehran, Iran*

Received 21 December 2009; accepted 27 January 2010
Published online in Wiley Online Library (wileyonlinelibrary.com).
DOI 10.1002/qua.22628

ABSTRACT: Quantum mechanics calculations were applied to investigate the N—H···O hydrogen bonding properties in linear $(urea)_{n=1-10}$ clusters. We investigated geometries, binding energies, and ^{17}O chemical shielding tensors of urea clusters, by means of MP2 and DFT methods. The charge-transfer character of the urea clusters was estimated using Natural Bonding Orbital characteristics. It was found that the cooperativity effects enhance significantly the N—H···O hydrogen bond from −33.08 (dimer) to −47.67 kJ/mol (decamer). The *n*-dependent trend of ^{17}O shielding tensors was reasonably correlated with cooperative effects in $r_{C=O}$ bond distance. To deepen the nature of the interaction in urea clusters, the scheme of decomposition of the interaction energies was applied using Morokuma analysis and a variant of symmetry-adapted perturbation theory (SAPT) based on DFT description of monomers, referred to as SAPT-DFT. The SAPT-DFT analysis of the interaction energy components indicates that the electrostatic and dispersive interactions are the most important attractive terms in the urea dimer. © 2010 Wiley Periodicals, Inc. Int J Quantum Chem 000: 000–000, 2010

Key words: hydrogen-bonding cooperativity; quantum mechanics; ^{17}O chemical shielding tensors; Morokuma analysis; symmetry-adapted perturbation theory

Correspondence to: N. L. Hadipour; e-mail: nas.hadipour@gmail.com

Additional Supporting Information may be found in the online version of this article.

© 2010 Wiley Periodicals, Inc.

1. Introduction

The importance of hydrogen-bonding interactions has been recognized in a wide range of chemical and biophysical phenomena. One particularly relevant aspect in the hydrogen-bonding theory is hydrogen bond cooperativity, which is typically described as nonadditive enhancement of a hydrogen bond through formation of another hydrogen bond with either a proton donor or proton acceptor [1]. As the equations of classical electrostatics include only pair-wise additive interactions of localized monomers, the existence of these effects can be considered as a departure from the classical electrostatics model of hydrogen-bonding (H-bonding), indicating the inadequacy of considering its electrostatics picture alone, and, perhaps even more important, suggesting the presence of significant electronic delocalization [2–5]. The cooperativity of H-bond plays an important role in controlling and regulating the processes occurring in biosystems [6–8]. Many physical and chemical properties of materials are determined by H-bonding cooperativity. For example, the cooperativity of hydrogen bond can stabilize secondary and tertiary structures of biomolecules and related assemblies. Influence of the cooperative effects on the H-bond properties was investigated recently using experimental microwave and theoretical techniques for $H_3N\cdots HF$ and $H_3N\cdots HF\cdots HF$ complexes [9]. It was found that addition of the second HF molecule to the $H_3N\cdots HF$ complex leads to a 0.21(6) Å reduction in the N···H hydrogen bond. In other words, the cooperativity effect exists in clusters where the monomer can participate concertedly as donor and acceptor. There are also numerous theoretical investigations on the cooperativity effect [10, 11]. For example, cooperativity in N—H···O=CNH hydrogen bond in benzamide [12] and acetamide [13] was investigated. Results indicated that cooperative effects enhance the H-bond strength and decrease the covalent nature of the proton donating bond. The effects are evidenced as an elongation and a red-shift in the corresponding stretching mode. In case of acetamide, cooperativity down-shifting was found for calculated ^{14}N nuclear quadrupole coupling constants. Kar and Scheiner [14] have just recently conducted a comparative study of the cooperativity in C—H···O and O—H···O hydrogen bonds. This work presents the rather interesting result that the cooperativity of C—H···O and O—H···O bonds is similar; although solvent effects, represented by a continuum with a dielectric constant, result in reduced cooperativity in all systems. There are other types of H-bonds, for example C—H···F, where an enhancement of blue shift is observed as a result of cooperativity [15]. Cooperativity may exist for different kinds of hydrogen bonds, so-called conventional and unconventional ones. There are very interesting π-hydrogen-bonded interactions analyzed at the MP2/6-311++G(2d,2p) level of approximation [16]. The other example where the H-bond cooperativity analyzed for chains of acetic acid molecules [17] is a very important contribution. It is found that a rather small cooperativity, 1.2 kcal/mol (at the HF/6-31G** level of theory), is present along the acetic acid molecules.

A number of theoretical investigations have been performed concerning cooperative effects on structural and spectroscopic parameters of H-bonds in model peptides [18–22]. Urea looks like a simple molecular model for presence of N—H···O hydrogen-bond cooperativity in gas phase (see Fig. 1). Owing to the importance of N—H···O interaction in protein and polypeptides stability, urea has received most attention from the theoretical [23–28] and experimental [29–32] points of view. In a previous article, Dannenberg et al. studied $(urea)_{1–10}$ containing intermolecular interactions [33]. They investigated only structural and energetic of clusters using HF, DFT, and MP2/D95** methods. To our knowledge, no studies have been performed on the cooperativity effects on ^{17}O chemical shielding tensors and charge transfer effects in the urea clusters. The application of the decomposition of the interaction energy to study the effect of cooperativity seems to be interesting. Such an attitude was not extensively applied to analyze that phenomenon in urea clusters. Furthermore, there has been little investigation of physical nature of N—H···O hydrogen bonds in the urea clusters and correlations between intermolecular components and molecular properties.

The aim of this work is to systematically examine properties of the N—H···O interaction in various $(urea)_{n=1–10}$ clusters based on MP2 and DFT methods. We will discuss the structural, energetical, and ^{17}O chemical shielding tensors of the clusters, H-bonding cooperativity, and its dependence on the cluster size. The Natural Bonding Orbital (NBO) analysis and decomposition scheme of the interaction energies are also applied here to

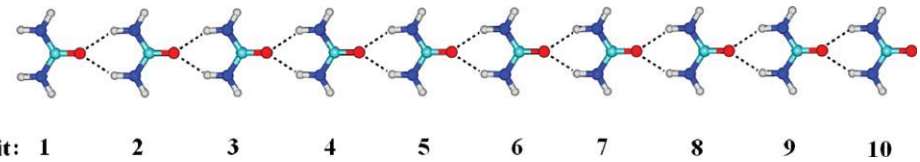

FIGURE 1. Geometry of $(urea)_{10}$ cluster optimized at B3LYP/6-311++G** level of theory. [Color figure can be viewed in the online issue, which is available at wileyonlinelibrary.com.]

deepen the nature of the N—H···O hydrogen bonds.

2. Computational Aspects

2.1. DFT AND MP2 CALCULATIONS

Molecular orbital calculations were performed using DFT and MP2 methods. All the computations were carried out using Gaussian 03 program [34]. The geometry optimization of $(urea)_{1-10}$ clusters were fully performed with subsequent frequency calculations using the B3LYP method and 6-311++G** basis set. Although geometries were not optimized, however, on the counterpoise-corrected (CP) surface [35], the interaction energies obtained at the MP2 and B3LYP levels were corrected for the basis set superposition error (BSSE)[35]. The BSSE corrected energies were determined by means of

$$\Delta E = E_n - \sum_i^n E_i \tag{1}$$

where E_n is the total energy of the cluster of size n and E_i is the energy of the individual monomers, in the cluster geometry, calculated using all the basis set of the cluster. The MP2 correlation method was used in consideration of the results presented by Novoa and Sosa [36] suggesting that this method provides a better description of the energetics of H-bonded complexes than DFT methods.

^{17}O chemical shielding calculations were performed using GIAO approach [37] at the B3LYP/6-311++G** level of theory. The calculated shielding eigenvalues (σ_{11}, σ_{22}, and σ_{33}) were used to obtain ^{17}O shielding isotropy, $\sigma_{iso} = \frac{1}{3}(\sigma_{11} + \sigma_{22} + \sigma_{33})$, and anisotropy parameters, $\Delta\sigma = \sigma_{33} - \frac{1}{2}(\sigma_{11} + \sigma_{22})$.

2.2. NATURAL BONDING ORBITAL ANALYSIS

Natural Bonding Orbital (NBO) analyses [38] were performed on wave functions calculated at the MP2/6-311++G** level. The NBO method corresponds closely to the picture of localized bonds and lone pairs as basic units of molecular structure. NBO analysis transforms the delocalized many-electron wave function into optimized electron pair bonding units, corresponding to the Lewis structure picture. Starting from a given input atomic orbital basis set $\{\varphi_i\}$, the program performs a series of transformations to form "natural" atomic orbitals (NAOs), natural hybrid orbitals (NHOs), natural bond orbitals (NBOs), and natural semilocalized molecular orbitals (NLMOs).

2.3. BINDING ENERGY DECOMPOSITION SCHEME

The following interaction energy components can be obtained in the Morokuma analysis [39, 40]: (1) electrostatic (EL), the classical columbic interaction of the occupied orbitals (occ) of one fragment (A) with those of another fragment (B); (2) EX, the interaction between occ(A) and occ(B) that causes electron delocalization between the two fragment occupied orbitals (this is often referred to as the exchange interaction); (3) polarization (PL), the interaction which causes the mixing of occ and virtual orbitals (vir) within each fragment; (4) charge transfer (CT), the interaction which causes the interfragment delocalization by mixing occ of one fragment with vir of another and vice versa; (5) MIX, the remaining term in the interaction energy. However, in the Morokuma approach, the total energy and its components are not free of BSSE. Hence, BSSE corrections were considered for calculation of the components and SCF energies. The polarization energy in this scheme may be approximately described as connected with the internal redistribution of electron charge, whereas the charge transfer term is connected with the density shifts from one molecule to the other. All the Morokuma decompositions were carried out using *GAMESS* package [41].

In addition to the Morokuma analysis, the symmetry-adapted perturbation theory (SAPT)

treatment [42] was also used and the SAPT-DFT calculations were performed by SAPT 2008 [43]. The method allows for the separation of the interaction energies into physically well-defined components, such as those arising from electrostatics, induction, dispersion, and exchange. The SAPT-DFT interaction energy ($E^{\text{SAPT-DFT}}$) is given by Eq. (2):

$$\begin{aligned} E_{\text{int}}^{\text{SAPT-DFT}} &= E_{\text{el}}^{(1)} + E_{\text{exch}}^{(1)} + E_{\text{ind}}^{(2)} + E_{\text{exch-ind}}^{(2)} \\ &\quad + E_{\text{disp}}^{(2)} + E_{\text{exch-disp}}^{(2)} \\ &= E_{\text{el}} + E_{\text{exch}} + E_{\text{ind}} + E_{\text{disp}} \end{aligned} \tag{2}$$

where

$$E_{\text{exch}} = E_{\text{exch}}^{(1)} + E_{\text{exch-ind}}^{(2)} + E_{\text{exch-disp}}^{(2)} \tag{3}$$

and the single terms in Eq. (2) describe the electrostatics, exchange-repulsion, induction, exchange-induction, dispersion, and exchange-dispersion terms, respectively. Because BSSE effects are explicitly included when the SAPT interaction energies are evaluated, a comparison of BSSE corrected supermolecular interaction energy and the SAPT interaction energy is appropriate.

3. Results and Discussion

3.1. EQUILIBRIUM GEOMETRIES

Although no symmetry was imposed during geometrical optimization, all of the optimized urea clusters have linear open chain structures as shown in Figure 1. For its isolated molecule, $r_{\text{C-N}} = 1.375$ Å, $r_{\text{N-H}} = 1.005$ Å, and $r_{\text{C=O}} = 1.220$ Å were obtained, which are in reasonable agreement with the experimentally deduced geometry for the urea monomer: $r_{\text{C-N}} = 1.378$ Å, $r_{\text{N-H}} = 0.998$ Å, and $r_{\text{C=O}} = 1.221$ Å [44].

As evidenced from Table I, the N—H bonds of the $(\text{urea})_{n=2-10}$ clusters fall into two categories: N—H of unit 1 and N—H of the others (unit $2 - n$) acting as H-bonding donors. Note that for the monomer and $(\text{urea})_{2-n}$ clusters, the r_{NH} values refer to the N—H hydrogen bond donors antipositioned toward the carbonyl oxygen. Relative to the N—H of isolated monomer (1.005 Å), N—H distances of unit 1 are approximately constant and those of $2 - n$ units are elongated. On the other hand, N—H distances of unit 1 do not exhibit any cooperative effect with growing cluster size. The average N—H lengths of unit $2 - n$ are as follows: 1.009 Å for dimer, 1.010 Å for trimer, 1.012 Å for tetramer, 1.012 Å for pentamer, 1.013 Å for hexamer, 1.013 Å for heptamer, 1.014 Å for octamer, 1.014 Å for nonamer, and 1.014 Å for decamer, respectively. The magnitude of the elongation decreases slightly as the number of molecules in cluster increases.

As C=O of unit n does not contribute in the H-bonding, its length for each cluster (n) is slightly increased compared with C=O distance (1.220 Å) of the isolated urea. For the other urea units, an increase in the $r_{\text{C=O}}$ bond lengths is generally observed upon enlarging the size of the cluster. The extent of the changes depends on the size of the cluster and on the position of the molecule within the cluster. On the other hand, the C—N bond lengths in $(\text{urea})_{n=2-10}$ clusters become smaller as the size of the cluster increases. The calculated $r_{\text{C-N}}$ length for central molecules in decamer model, 1.359 Å, differs from monomer value by 0.016 Å.

It can be seen from Table I that intermolecular N—H···O bonds are also notably altered by the cooperative nature of hydrogen bond. It is seen that adding a third molecule reduces considerably $r_{\text{O···H}}$ value by 0.045 Å. The average values of $r_{\text{N-H···O}}$ for the clusters (n = 3–10) are 0.022 (2.19%), 0.035 (3.53%), 0.043 (4.32%), 0.049 (4.86%), 0.053 (5.25%), 0.056 (5.55%), 0.058 (5.78%), 0.059 (5.94%) shorter than the dimer (2.146 Å), respectively. What is more, the contraction in the $n = 10$ cluster is more than 200% of the $n = 3$, reflecting the strongly cooperative effects in the $(\text{urea})_{n=1-10}$ clusters and its progressive enhancement with the monomer number.

Therefore, the n-dependent variation in structural parameters should serve as a useful signature of H-bonding cooperativity of urea clusters. Calculated cooperative effects in the urea chains can be compared with other H-bonded systems. All mentioned results for urea clusters are compatible to those obtained at the DFT levels for formamide [45, 46], acetamide [13], *N*-methylformamide [47], polyalanine chains in α-helical and extended structure [48, 49], and antiparallel β-sheet models [50].

3.2. ENERGETICS

Calculated H-bonding interaction energies of the fully optimized linear urea clusters, at the

TABLE I

Structural properties of (urea)$_n$ clusters calculated at B3LYP/6-311++G level.**

Parameter	$n=1$	$n=2$	$n=3$	$n=4$	$n=5$	$n=6$	$n=7$	$n=8$	$n=9$	$n=10$
r_{N-H}	1.005	1.005	1.005	1.005	1.005	1.006	1.006	1.006	1.006	1.006
		1.009	1.010	1.011	1.011	1.011	1.012	1.012	1.012	1.012
			1.011	1.013	1.013	1.013	1.014	1.014	1.014	1.014
				1.012	1.013	1.014	1.014	1.014	1.015	1.015
					1.012	1.014	1.014	1.015	1.015	1.015
						1.012	1.014	1.014	1.015	1.015
							1.012	1.014	1.015	1.015
								1.012	1.014	1.015
									1.012	1.014
										1.012
$r_{C=O}$	1.220	1.228	1.231	1.232	1.232	1.232	1.233	1.233	1.233	1.233
		1.225	1.235	1.238	1.239	1.240	1.240	1.240	1.240	1.240
			1.225	1.237	1.240	1.241	1.242	1.242	1.242	1.242
				1.227	1.238	1.241	1.242	1.243	1.243	1.243
					1.227	1.238	1.242	1.243	1.243	1.244
						1.228	1.239	1.242	1.243	1.244
							1.228	1.239	1.242	1.243
								1.228	1.239	1.242
									1.228	1.239
										1.228
r_{C-N}	1.375	1.368	1.366	1.365	1.365	1.365	1.365	1.365	1.365	1.365
		1.374	1.364	1.362	1.362	1.361	1.361	1.361	1.361	1.361
			1.373	1.363	1.361	1.360	1.360	1.360	1.360	1.360
				1.372	1.363	1.361	1.360	1.359	1.359	1.359
					1.372	1.363	1.360	1.360	1.359	1.359
						1.372	1.362	1.360	1.359	1.359
							1.372	1.362	1.360	1.359
								1.372	1.362	1.360
									1.372	1.362
										1.372

B3LYP/6-311++G** and MP2/6-311++G** levels of theory, are presented in Table II. The deviation of the average binding energy from that of dimer is another indication of hydrogen bond cooperativity. Both B3LYP and MP2 calculations predict that for the urea clusters, cooperative effects tend

TABLE II

Calculated average values of binding energies, ΔE_e, association energies, $\Delta E_{en,n-1}$, and BSSE corrected binding energies, ΔE_e^{CP}, with 6-311++G basis set for (urea)$_{n=2-10}$ clusters.**[a]

Parameter	Method	$n=2$	$n=3$	$n=4$	$n=5$	$n=6$	$n=7$	$n=8$	$n=9$	$n=10$	$n=\infty$
ΔE_e	B3LYP	−35.55	−40.57	−43.53	−45.46	−46.75	−47.72	−48.47	−49.01	−49.47	−52.71
	MP2	−39.60	−44.33	−47.09	−48.89	−50.10	−50.98	−51.69	−52.19	−52.19	−55.65
$\Delta E_{en,n-1}$	B3LYP	−35.55	−45.63	−49.43	−51.15	−52.02	−52.53	−52.82	−53.03	−53.15	−58.66
	MP2	−39.60	−49.05	−52.65	−54.24	−55.04	−55.45	−55.75	−55.91	−56.00	−61.26
ΔE_e^{CP}	B3LYP	−33.08	−39.23	−42.20	−44.12	−45.12	−46.13	−46.88	−47.17	−47.67	−51.31
	MP2	−34.81	−39.18	−41.69	−43.32	−44.43	−45.25	−45.86	−46.34	−46.59	−49.47
Cooperativity	B3LYP	—	−6.15	−9.12	−11.04	−12.04	−13.05	−13.80	−14.09	−14.60	−18.23
	MP2	—	−4.37	−6.88	−8.51	−9.62	−10.44	−11.05	−11.53	−11.78	−14.66

[a] All calculated energies in kJ/mol.

to increase intermolecular binding energies. These results are in complete agreement with previous theoretical work at the B3LYP and MP2/D95** levels of theory [33]. Cooperative enhancement stabilizes the average H-bond interaction (ΔE_e) in the decamer by about −49.47 and −52.61 kJ/mol, at the B3LYP and MP2 levels, which are equivalent to adding −13.92 and −13.01 kJ/mol to the dimer H-bonding energy, respectively.

Trends in the stabilization of ΔE_e with increasing chain length can be appreciated by extrapolation of the average H-bonding energy versus $1/n$, where n is the number of molecules in the cluster; a perfect linear correlation is found in this case [Eq. (4)]:

$$\Delta E_e = 35.20(1/n) - 52.71 \quad [\text{B3LYP}] \qquad (4)$$

$$\Delta E_e = 32.89(1/n) - 55.65 \quad [\text{MP2}]$$

that indicates that the ΔE_e approaches −52.71 and −55.65 kJ/mol values as $n \to \infty$, respectively. The ΔE_e is increased by 48% at the B3LYP and 40% at the MP2 levels of theory, which are smaller than the extrapolated percent increase in the one dimensional chains of formamide molecules (200%) [45], but larger than those of acetamide molecules (31%) [13]. The ordering of cooperativity enhancement in the ΔE_e calculated for formamide (−54.32 kJ/mol) [45] and acetamide (−21.92 kJ/mol) [13] supports the view that the degree of cooperativity is proportional to the strength of N—H···O hydrogen bond.

Table II reveals also the energy changes by addition of one monomer to the $(\text{urea})_{n-1}$ cluster according to urea + $(\text{urea})_{n-1} \rightarrow (\text{urea})_n$ reaction. It must be mentioned that with no cooperative effects, energy of the process would have been constant and identical to the binding energy of the dimer. However, Table II predicts, at the B3LYP/6-311++G** level, a 17.60 kJ/mol cooperative enhancement from dimer to decamer cluster which means a 50% increase with respect to the dimer binding energy. These cooperative effects become less significant by cluster enlargement. However, the extrapolated value suggests that the $\Delta E_{e,n,n-1}$ of infinite urea chain is about 65% greater than dimer value.

The importance of BSSE correction on the cooperative effects was also studied. The magnitude of the BSSE can be judged by comparing the H-bonding energies, ΔE_e, and corrected binding energy, ΔE_e^{CP}, values. As Table II indicates, at both levels of theory, the CP correction for the all cases is about 1.3–6.0 kJ/mol. Considering the values mentioned above, the percentage of cooperative enhancement would be quite similar for corrected and uncorrected values. Therefore, it can be concluded that BSSE has no important role in studying the cooperative effects.

3.3. ^{17}O CHEMICAL SHIELDING TENSORS

The ^{17}O chemical shielding tensors were calculated at the B3LYP/6-311++G** level of theory. Table III indicates the calculated ^{17}O shielding isotropic, σ_{iso}, and anisotropic, $\Delta\sigma$, values of $(\text{urea})_{n=1-10}$ clusters (the ^{17}O shielding principal components are shown in the Supporting Information).

The intermolecular hydrogen bonds are expected to strongly affect electronic environment at the H-bonded nuclei. Thus, the cooperative effects in electronic structure induced by N—H···O hydrogen-bond formation affect the ^{17}O chemical shielding tensors in $(\text{urea})_n$ clusters. As shown in Table III, all of the ^{17}O nuclei acting as H-acceptors are shielded relative to the ^{17}O nucleus of the isolated urea molecule (σ_{iso} = 28.85 ppm). However, the magnitude of the shielding is more significant for interior units. The calculated ^{17}O shielding tensors of clusters (n = 2–10) fall into two categories: ^{17}O shielding of end unit n (viz. the right terminal unit) and ^{17}O shielding of the others [unit 2-(n-1)] acting as H-acceptors. The σ_{iso} parameter of the right terminal unit (viz. unit n) for n = 3–10 decrease relative to those the dimer. Clearly, the interaction between interior units is much stronger than those at the two ends. This is because the interior monomer unit of the general urea···urea chain plays either as an H-bond donor or acceptor. However, we note that the σ_{iso} values for the interior units deviate significantly from those of the end units. Figure 2 indicates the σ_{iso} behavior versus urea molecule position in the n = 10 chain. As a matter of fact, for $(\text{urea})_{10}$ cluster the most deviation from dimer values is observed for interior units. The magnitude of the deviation for unit n in each cluster is gradually diminished from the dimer to the decamer cluster.

Moreover, it can be observed that the average ^{17}O shielding isotropy values for H-bonded C=O units of the chains ($n > 2$) are as follows: 56.01 ppm for trimer, 60.76 ppm for tetramer, 63.70 ppm for pentamer, 65.81 ppm for hexamer, 67.29 ppm for heptamer, 68.39 ppm for octamer, 69.25 ppm for nonamer, and 69.87 ppm for decamer,

TABLE III

^{17}O isotropic and anisotropic shielding values (in ppm) of urea clusters at B3LYP/6-311++G level.**

Parameter	n =1	n = 2	n = 3	n = 4	n = 5	n = 6	n = 7	n = 8	n = 9	n = 10
σ_{iso}	28.85	47.95	53.41	55.54	56.54	57.09	57.45	57.71	57.92	58.08
		38.53	58.61	64.27	66.43	67.46	68.05	68.42	68.70	68.85
			42.45	62.47	68.13	70.29	71.32	71.91	72.29	72.51
				44.00	63.96	69.60	71.76	72.79	73.37	73.70
					44.70	64.61	70.23	72.38	73.40	73.93
						45.04	64.90	70.50	72.64	73.61
							45.22	65.04	70.61	72.68
								45.32	65.09	70.55
									45.37	64.96
										45.32
$\Delta\sigma$	404.55	350.34	337.41	332.71	330.98	330.29	330.06	330.06	330.18	330.38
		376.86	316.52	301.77	296.79	294.83	294.04	293.76	293.74	293.55
			369.64	306.94	291.61	286.42	284.37	283.54	283.24	283.10
				366.61	302.99	287.36	282.07	279.98	279.12	278.76
					365.15	301.01	285.19	279.85	277.74	276.83
						364.34	299.85	283.91	278.52	276.35
							363.81	299.08	283.02	277.53
								363.44	298.51	282.18
									363.15	297.68
										362.40

respectively. On the other hand, the magnitude of the shielding of ^{17}O nuclei for each cluster first progressively increases from the left unit to the right and then decreases. As a matter of fact, the average shifts of ^{17}O shielding anisotropy values from the dimer for units for n = 3–10 are 22.41 (6.2%), 36.59 (10%), 46.10 (12.7%), 52.89 (14.5%), 57.97 (15.9%), 61.90 (17%), 65.02 (17.9%), and 67.72 (18.6%), respectively. Clearly, the downshift in decamer is about three times that for the dimer. Therefore, the n-dependent variation in ^{17}O shielding tensor should serve as a useful signature of H-bond cooperativity of the urea clusters. This indicates that, in agreement with the previous sections, the ^{17}O shielding shift at size n = 10 seems to arrive at saturation.

3.4. CHARGE TRANSFER

In terms of NBO theory [51], A—H···B hydrogen bonding can be attributed to the localized $n_B \rightarrow \sigma^*_{AH}$ interaction due to electronic delocalization from the filled lone pair n(B) of "electron donor" B into the unfilled antibond σ^* (A—H) of "electron acceptor" A—H. Stabilization energy, E(2), reflects the attractive interaction in the A—H···B bonding and thus can be used to characterize the strength of the A—H···B bond. For each electron donor NBO (i) and acceptor NBO (j), E(2) associated with delocalization $i \rightarrow j$ is estimated as

$$E(2) = \Delta E_{ij} = c_i \frac{F_{ij}^2}{\varepsilon_j - \varepsilon_i} \quad (5)$$

where c_i is donor orbital occupancy, ε_i and ε_j are orbital energies, and F_{ij} is the off-diagonal NBO Fock matrix element.

The orbital overlap between n_O and N—H antibonding, σ^*_{N-H}, is associated with the formation

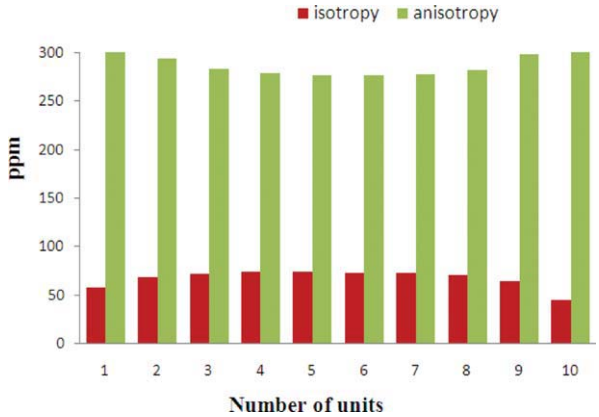

FIGURE 2. Calculated NMR parameters for $(urea)_{10}$ cluster. [Color figure can be viewed in the online issue, which is available at wileyonlinelibrary.com.]

of intermolecular N—H···O hydrogen bond. The overlap and the corresponding charge transfer (CT) lead to energetic stabilization of the H-bonded systems. Hence it offers us a theoretical basis to characterize the H-bond strength. Table IV shows considerable cooperativity in some characteristics of delocalization energy $E(2)$, the amount of transferred charge ($q_{n_O \rightarrow \sigma NH^*}$) and Fock matrix elements (F_{ij}) along the different $(urea)_n$ clusters. The calculated delocalization energy for $n_O \rightarrow \sigma^*_{NH}$ interaction of dimer is 2.06 kcal/mol, at the MP2/6-311++G**. This energy increases to 2.56 and 2.63 kcal/mol in trimer, which is in accordance with other evidences for intermolecular hydrogen bond strength increase. The average values of F_{ij} per monomer from $n = 2$–10 are 0.053, 0.060, 0.063, 0.066, 0.068, 0.070, 0.071, 0.072, and 0.072 au, respectively. Very clearly, the increased average shows that the H-bond strength enhances with the cluster size. However, we also note that this increment from n to $n + 1$ decays gradually with cluster size enlarging. For example, the increment from dimer to trimer is 0.007 au, whereas the corresponding increment from octamer to the nonamer and decamer is 0.001 au. It is also expected that interior urea units of general N—H···O=CNH···N—H chain be left approximately electroneutral by simultaneous charge transfer. When a small quantity of charge is transferred between the two urea molecules, in No. 1 → No. 2 sense, molecule No. 2 acquires slight anionic character. This raises the energy of its filled orbitals and renders them more spatially diffuse. On the other hand, the No.1 molecule acquires slight cationic property, rendering it better acceptor. Furthermore, the acceptor No. 2, in No. 1 → No. 2 interaction, inherently becomes an improved donor for concerted No. 1 → No. 2 → No. 3 interactions.

The charge transfer (q_{HB}) of urea monomers as a consequence of the $n_O \rightarrow \sigma^*_{N-H}$ interaction between n_O to N—H antibonding, σ^*_{N-H}, can be used to characterize the amount of cooperative effects in the urea clusters. Recently, it has been widely shown that for H-bonded clusters, the calculated q_{HB} values reasonably correlate with the number of monomer in the cluster [52, 53]. However, the results collected in Table IV show that the calculated q_{HB} value for central units of decamer cluster (4.14×10^{-3} au) is more than 200% of the dimer (1.92×10^{-3} au), reflecting the strong cooperative effects in the linear urea clusters. A correlation between $\ln(E_{n_O \rightarrow \sigma^*_{N-H}})$ and $R_{N-H...O}$

TABLE IV

NBO analysis of donor-acceptor interactions in $(urea)_{n=2-10}$ clusters showing Fock matrix interaction elements F_{ij}, stabilization $E(2)$ values, and charge-transfer $q_{n_O \rightarrow \sigma NH^*}$ calculated at MP2/6-311++G level.**

n	O···H	F_{ij}	$E(2)$	$q_{n_O \rightarrow \sigma NH^*}$
2	1···2	0.053	2.06	1.92
3	1···2	0.059	2.56	2.41
	2···3	0.060	2.63	2.52
4	1···2	0.061	2.77	2.61
	2···3	0.067	3.35	3.18
	3···4	0.062	2.85	2.69
5	1···2	0.062	2.85	2.69
	2···3	0.070	3.61	3.47
	3···4	0.070	3.63	3.47
	4···5	0.063	2.94	2.78
6	1···2	0.063	2.89	2.78
	2···3	0.071	3.71	3.57
	3···4	0.073	3.93	3.78
	4···5	0.071	3.75	3.57
	5···6	0.064	2.99	2.87
7	1···2	0.063	2.91	2.78
	2···3	0.071	3.77	3.57
	3···4	0.074	4.04	3.88
	4···5	0.074	4.05	3.93
	5···6	0.072	3.81	3.72
	6···7	0.064	3.01	2.87
8	1···2	0.063	2.92	2.78
	2···3	0.072	3.08	3.67
	3···4	0.074	4.10	3.93
	4···5	0.075	4.18	4.03
	5···6	0.074	4.11	3.93
	6···7	0.072	3.84	3.67
	7···8	0.064	3.02	2.87
9	1···2	0.063	2.92	2.78
	2···3	0.072	3.82	3.67
	3···4	0.075	4.13	4.03
	4···5	0.075	4.24	4.03
	5···6	0.076	4.25	4.14
	6···7	0.076	4.15	4.14
	7···8	0.072	3.86	3.67
	8···9	0.064	3.03	2.87
10	1···2	0.063	2.93	2.78
	2···3	0.072	3.081	3.67
	3···4	0.075	4.31	4.03
	4···5	0.076	4.25	4.14
	5···6	0.076	4.28	4.14
	6···7	0.076	4.26	4.14
	7···8	0.075	4.14	4.03
	8···9	0.072	3.85	3.67
	9···10	0.064	3.03	2.87

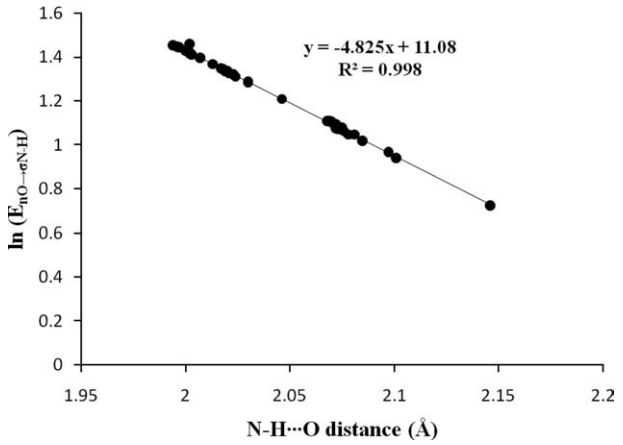

FIGURE 3. Correlation of $\ln(En_O \rightarrow \sigma^*_{NH})$ with hydrogen bond distance ($R_{N-H\cdots O}$).

distances for 45 H-bonds of the equilibrium geometries is also found as follows (see Fig. 3):

$$\ln(En_O \rightarrow \sigma^*_{N-H}) = -4.825\ R_{N-H\cdots O} + 11.08 \quad (R_2 = 0.998) \tag{6}$$

that indicates the $E_{n_O \rightarrow \sigma^*_{N-H}}$ stabilization energy contributes mainly to the cooperativity of N—H···O hydrogen bond. In principle, the shift in electron density rather than being localized over a particular regain delocalizes throughout the acceptor and donor molecules. Therefore, the net charges (q_{CT}) distributed over the monomer units due to the shifts in electron densities were also evaluated. No correlation was obtained between the q_{HB} and q_{CT} values for the linear urea clusters. In this case, it was found that the net charges on the two terminal units are slowly negative and the charges on the interior units are almost positive.

3.5. BINDING ENERGY DECOMPOSITION SCHEME

The results of Tables V show the interaction energy components of urea clusters calculated within the Morokuma scheme [39, 40]. These results are presented to check the well-known statements that the cooperativity is connected with the charge transfer interaction energy term [54]. Table V shows the variation of all energy terms if the number of urea monomers in the cluster increases. More specifically, it is apparent that from dimer to decamer cluster the average value of EL, EX, PL, and CT terms increase by 4.61 (36%), 4.06 (71%), 2.71 (150%), and 1.17 (56%) kJ/mol, respectively. Extrapolations to $n = \infty$ lead to following approximated values for the infinite extended urea cluster: EL = −77.93, EXCH = 44.42, PL = −21.33, and CT = −14.70 kJ/mol. A detailed analysis of the interaction energy allows us to classify the studied urea clusters as belonging to the class of middle strong HBs. The following ratios are analyzed here, CT/EL, PL/EL, and (CT + PL)/EL and their correlations with N—H···O distance are presented (see Fig. 4). The linear correlation coefficients for these three dependencies are equal to 0.999. One can see that not only the charge transfer energy depends on the N—H···O distance but also the polarization energy term. The second term depends on the N—H···O distance even more because the polarization/electrostatic ratio increases more than the

TABLE V
Morokuma decomposition of interaction energies of linear urea clusters.[a,b]

n	EL	EX	PL	CT	MIX	E_{SCF}
2	−54.24	23.80	−7.49	−8.74	−0.59	−41.86
3	−61.02	28.94	−11.21	−10.33	−0.71	−54.12
4	−64.99	32.70	−13.63	−11.38	−0.84	−58.13
5	−67.71	35.17	−15.26	−12.04	−0.92	−60.76
6	−69.59	36.97	−16.39	−12.59	0.96	−62.56
7	−71.01	38.31	−17.27	−12.96	−0.96	−63.90
8	−72.10	39.35	−17.90	−13.22	−1.00	−64.90
9	−72.93	40.15	−18.44	−13.47	−1.00	−65.70
10	−73.52	40.77	−18.82	−13.63	−1.05	−66.24
∞	−77.93	44.42	−21.33	−14.70	−2.99	−72.53

[a] All terms in kJ/mol.
[b] Average values for $n > 2$ clusters.

charge transfer/electrostatic ratio if the N—H···O distance decreases. Furthermore, there is the MIX interaction energy term within the Morokuma scheme which is the result of nonseparated components. These results show that the cooperativity effect enhances H-bond interaction and hence the covalency of this interaction. The covalency is related to the greater importance of the delocalization energy (polarization and charge transfer) and less importance of electrostatic energy. That may be supported if one relates to the recent statements that the electrostatic interaction is overestimated as computed at the Hartree-Fock level at which there is a too stabilizing electrostatic interaction at the cost of covalency.

Figure 5 shows the CCSD(T) binding energies and SAPT-DFT interaction energy components as a function of the intermonomer separation. The SAPT-DFT provides decomposition of the interaction energy and an estimation of specific contributions related to the physical concepts such as dispersion and induction energies. It can be seen that the SAPT interaction energies are in relatively good agreement with those determined using CCSD(T). This figure also shows clearly that various contributions have different distance dependences. The exchange energy term, which arises from the short-range Pauli's repulsion, is most sensitive to variations of the H-bond distance. Both induction and dispersion contributions are

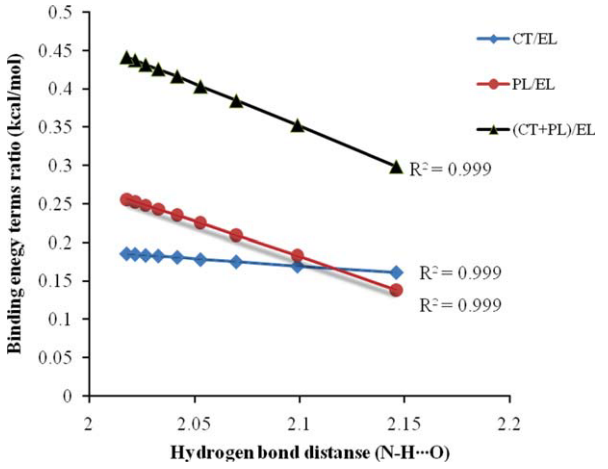

FIGURE 4. Correlation between H···O distance (Å) and the ratio of the average interaction energy terms: charge transfer/electrostatic (CT/EL), polarization/electrostatic (PL/EL), and polarization and charge transfer/electrostatic [(CT + PL)/EL]. [Color figure can be viewed in the online issue, which is available at wileyonlinelibrary.com.]

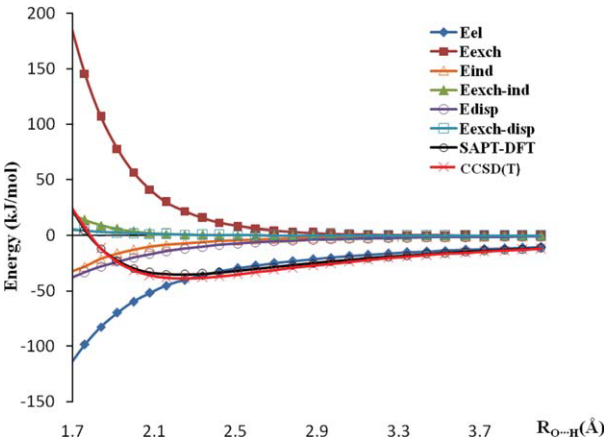

FIGURE 5. The SAPT-DFT binding energy components and CCSD(T) binding energies of the urea dimmer. [Color figure can be viewed in the online issue, which is available at wileyonlinelibrary.com.]

much less distance-dependent than the electrostatic and exchange terms. One of the most interesting aspects of the data depicted in Figure 5 is the increasing contribution of the electrostatic interaction to the overall stability of the complex with decreasing hydrogen bond distance. In the position of the potential energy minimum, the total SAPT-DFT interaction energy of the urea dimer is −34.67 kJ/mol. We have estimated the electrostatic energy (−46.42 kJ/mol), the exchange energy (31.91 kJ/mol), the induction energy (−8.61 kJ/mol), the dispersion energy (−14.47 kJ/mol) with exchange-induction effect (1.63 kJ/mol), and the exchange-dispersion energy (1.25 kJ/mol) of the urea dimer utilizing the aug-cc-pVDZ basis set. In complete agreement with other H-bonded clusters, the major attractive contribution to the total interaction energy emerges from the electrostatic with its contribution being nearly three times as large as the corresponding contribution from dispersion $E^{(2)}_{\mathrm{disp}}$, and six times as large as the corresponding contribution from induction $\mathrm{E}^{(2)}_{\mathrm{ind}}$.

4. Conclusion

This work reports MP2, DFT, NBO, and SAPT-DFT theories to investigate properties of N—H···O hydrogen bonding in linear H-bonded $(\mathrm{urea})_n$ clusters (n = 1–10) such as equilibrium geometries, binding energies, ^{17}O chemical shielding tensor, and $n_{\mathrm{O}} \rightarrow \sigma^{*}_{\mathrm{N-H}}$ charge transfer. The

contraction of N—H···O hydrogen bonding in the $n = 10$ cluster is more than 200% of the $n = 3$, reflecting the strongly cooperative effects in the $(urea)_{n=1-10}$ clusters and its progressive enhancement with the monomer number. Based on the MP2/6-311++G** calculations, we found 4.37 kJ/mol more stable in trimer cluster, due to the formation of the second hydrogen bond. All of the ^{17}O nuclei acting as H-acceptors are shielded relative to the ^{17}O nucleus of the isolated urea molecule ($\sigma_{iso} = 28.85$ ppm). However, the magnitude of the shielding is more significant for interior units. The calculated delocalization energy of $n_O \rightarrow \sigma^*_{N-H}$ interaction increases with number of urea molecules in the cluster. Such cooperative effects help to rationalize the common occurrence of N—H···O type H-bonding interactions in the biosystems. According to the SAPT-DFT analyses, we have estimated the electrostatic energy (−46.42 kJ/mol), the exchange energy (31.91 kJ/mol), the induction energy (−8.61 kJ/mol), the dispersion energy (−14.47 kJ/mol) with exchange-induction effect (1.63 kJ/mol), and the exchange-dispersion energy (1.25 kJ/mol) of the urea dimer utilizing the aug-cc-pVDZ basis set. Also, the calculated SAPT interaction energies are in relatively good agreement with those determined using CCSD(T).

References

1. Elrodt, M. J.; Saykally, R. J. Chem Rev 1994, 94, 1975.
2. Del Bene, J. E.; Pople, J. A. Chem Phys Lett 1969, 4, 426.
3. Van der Vaart, A.; Merz, K. M. Int J Quantum Chem 2000, 77, 27.
4. Rincon, L.; Almeida, R.; Aldea, D. G. Int J Quantum Chem 2005, 102, 443–453.
5. Clementi, E.; Kolos, W.; Lie, G. C.; Ranghino, G. Int J Quantum Chem 1980, 17, 377.
6. Guo, H.; Gresh, N.; Roques, B. P.; Salahub, D. R. J Phys Chem B 2000, 104, 9746.
7. Zhao, Y. L.; Wu, Y. D. J Am Chem Soc 2002, 124, 1570.
8. Wieczorek, R.; Dannenberg, J. J. J Am Chem Soc 2003, 125, 8124.
9. Hunt, S. W.; Higgins, K. J.; Craddock, M. B.; Brauer, C. S.; Leopold, K. R. J Am Chem Soc 2003, 125, 13850.
10. Scheiner, S. Hydrogen Bonding: A Theoretical Perspective; Oxford University Press: New York, 1997.
11. Kar, T.; Scheiner, S. J Chem Phys 2003, 119, 1473.
12. Esrafili, M. D.; Behzadi, H.; Hadipour, N. L. Chem Phys 2008, 348, 175.
13. Esrafili, M. D.; Behzadi, H.; Hadipour, N. L. Theor Chem Acc 2008, 121, 135.
14. Karr, T.; Scheiner, S. J Phys Chem A 2004, 108, 9161.
15. Karpfen, A.; Kryachko, E. S. J Phys Chem A 2005, 109, 8930.
16. DuPré, D. B.; Yappert, C. J Phys Chem A 2002, 106, 567.
17. Rovira, C.; Novoa, J. J. J Chem Phys 2000, 113, 9208.
18. Ludwig, R.; Weinhold, F.; Farrar, T. C. J Phys Chem A 1997, 101, 8861.
19. Ludwig, R.; Weinhold, F.; Farrar, T. C. J Chem Phys 1997, 107, 499.
20. Parker, L. L.; Houk, A. R.; Jensen, J. H. J Am Chem Soc 2006, 128, 9863.
21. Schlund, S.; Mladenovic, M.; Janke, E. M. B.; Engels, B.; Weisz, K. J Am Chem Soc 2005, 127, 16151.
22. Ireta, J.; Neugebauer, J.; Scheffler, M.; Rojo, A.; Galvan, M. J Phys Chem B 2003, 107, 1432.
23. Benkova, Z.; Černušak, I.; Zahradnik, P. Int J Quantum Chem 2007, 107, 2133.
24. Sun, H.; Kung, P. W.-C. J Comput Chem 2005, 26, 169.
25. Civalleri, B.; Doll, K.; Zicovich-Wilson, C. M. J Phys Chem B 2007, 111, 26.
26. Parra, R. D.; Ohlssen, J. J Phys Chem A 2008, 112, 3492.
27. Masunov, A.; Dannenberg, J. J. J Phys Chem A 1999, 103, 178.
28. Pal, S.; Manna, A. K.; Pati, S. K. J Chem Phys 2008, 129, 204301.
29. Kassi, S.; Petitperz, D.; Wlodarczak, G. J Mol Spectrosc 2004, 228, 293.
30. Vaughan, P.; Donohue, J. Acta Crystallogr 1952, 5, 530.
31. Worsham, J. E.; Levy, H. A.; Peterson, S. W. Acta Crystallogr 1957, 10, 319.
32. Dong, S.; Ida, R.; Wu, G. J Phys Chem A 2000, 104, 11194.
33. Masunov, A.; Dannenberg, J. J. J Phys Chem B 2000, 104, 806.
34. Frisch, M. J.; Trucks, G. W.; Schlegel, H. B.; Scuseria, G. E.; Robb, M. A.; Cheeseman, J. R.; Zakrzewski, V. G.; Montgomery, J. A.; Stratmann, R. E.; Burant, J. C.; Dapprich, S.; Millam, J. M.; Daniels, A. D.; Kudin, K. N.; Strain, M. C.; Farkas, O.; Tomasi, J.; Barone, V.; Cossi, M.; Cammi, R.; Mennucci, B.; Pomelli, C.; Adamo, C.; Clifford, S.; Ochterski, J.; Petersson, G. A.; Ayala, P. Y.; Cui, Q.; Morokuma, K.; Malick, D. K.; Rabuck, A. D.; Raghavachari, K.; Foresman, J. B.; Cioslowski, J.; Ortiz, J. V.; Stefanov, B. B.; Liu, G.; Liashenko, A.; Piskorz, P.; Komaromi, I.; Gomperts, R.; Martin, R. L.; Fox, D. J.; Keith, T.; Al-Laham, M. A.; Peng, C. Y.; Nanayakkara, A.; Gonzalez, C.; Challacombe, M.; Gill, P. M. W.; Johnson, B.; Chen, W.; Wong, M. W.; Andres, J. L.; Head-Gordon, M.; Replogle, E. S.; Pople, J. A. Gaussian 2003, revision B; Gaussian, Inc.: Pittsburgh, PA, 2003.
35. Boys, S. F.; Bernardi, F. Mol Phys 1970, 19, 553.
36. Novoa, J. J.; Sosa, C. J Phys Chem 1995, 99, 15873.
37. Wolinski, K.; Hilton, J. F.; Pulay, P. J Am Chem Soc 1990, 112, 8251.
38. Foster, J. P.; Weinhold, F. J Am Chem Soc 1980, 102, 7211.
39. Kitaura, K.; Morokuma, K. Int J Quantum Chem 1976, 55, 1236.
40. Morokuma, K.; Kitaura, K. In Chemical Applications of Atomic and Molecular Electrostatic Potentials; Politzer, P.; Truhlar, D. G., Eds.; Plenum: New York, 1981; p 215.
41. Schmidt, M. W.; Baldridge, K. K.; Boatz, J. A.; Elbert, S. T.; Gordon, M. S.; Jensen, J. H.; Koseki, S.; Matsunaga, N.;

Nguyen, K. A.; Su, S. J.; Windus, T. L.; Dupuis, M.; Montgomery, J. A. J Comput Chem 1993, 14, 1347.

42. Jeziorski, B.; Moszyñski, R.; Szalewicz, K. Chem Rev 1994, 94, 1887.
43. Bukowski, R.; Cencek, W.; Jankowski, P.; Jeziorski, B.; Jeziorska, M.; Kucharski, S. A.; Lotrich, V. F.; Misquitta, A. J.; Moszyñski, R.; Patkowski, K.; Podeszwa, R.; Rybak, S.; Szalewicz, K.; Williams, H. L.; Wheatley, R. J.; Wormer, P. E. S.Zuchowski, P. S. SAPT2008: An Ab Initio Program for Many-Body Symmetry-Adapted Perturbation Theory Calculations of Intermolecular Interaction Energies; University of Delaware and University of Warsaw, 2008.
44. Brown, R. D.; Godfrey, P. D.; Storey, J. J Mol Spectrosc 1975, 58, 445.
45. Vargas, R.; Garza, J.; Friesner, R. A.; Stern, H.; Hay, B. P.; Dixon, D. A. J Phys Chem A 2001, 105, 4963.
46. Kobko, N.; Dannenberg, J. J. J Phys Chem A 2003, 107, 10389.
47. Martínez, A. G.; Vilar, E. T.; Fraile, G.; Martínez-Ruiz, P. J Chem Phys 2006, 124, 23435.
48. Ireta, J.; Neugebauer, J.; Scheffler, M.; Rojo, A.; Galván, M. J Phys Chem B 2003, 107, 1432.
49. Wieczorek, R.; Dannenberg, J. J. J Am Chem Soc 2003, 125, 8124.
50. Viswanathan, R.; Asensio, A.; Dannenberg, J. J. J Phys Chem A 2004, 108, 9205.
51. Reed, A. E.; Curtiss, L. A.; Weinhold, F. Chem Rev 1988, 88, 899.
52. Song, H.; Xiao, H.; Dong, H. J Phys Chem A 2006, 110, 6178.
53. Song, H.-J.; Xiao, H.-M.; Dong, H.-S.; Zhu, W.-H. J Phys Chem A 2006, 110, 2225.
54. Desiraju, G. R. Acc Chem Res 2002, 35, 565.